Effects of Clay Dispersion and Content on the Rheological, Mechanical Properties, and Flame Retardance of HDPE/Clay Nanocomposites

Y. H. Lee,[1] Chul B. Park,[2] M. Sain,[1] M. Kontopoulou,[3] Wenge Zheng[2]

[1]*Centre for Biocomposites and Biomaterials Processing, Faculty of Forestry, University of Toronto, Ontario, Canada M5S 3B3*
[2]*Microcellular Plastics Manufacturing Laboratory, Department of Mechanical and Industrial Engineering, University of Toronto, Toronto, Ontario, Canada M5S 3G8*
[3]*Department of Chemical Engineering, Queen's University, Kingston, Ontario, Canada K7L 3N6*

Received 16 June 2006; accepted 21 February 2007
DOI 10.1002/app.26403
Published online 1 May 2007 in Wiley InterScience (www.interscience.wiley.com).

ABSTRACT: Full exfoliation of clay/high density polyethylene (HDPE) nanocomposites was successfully achieved with the aid of maleated HDPE (PE-*g*-MAn), by melt blending in a twin-screw extruder employing a long residence time configuration. The morphology of the composites was determined using wide-angle X-ray diffraction and transmission electron microscopy. The effects of clay content and state of clay dispersion on the rheological, tensile properties, and flame retardancy of nanocomposites containing very small amounts of clay, in the range of 0.05–1.0 wt %, were investigated in this study. It was demonstrated that achieving a higher degree of exfoliation for nanosized clay particles is key to enhancing the rheological, mechanical, and flame retarding properties even when small amounts of clay (less than 1%) are used. © 2007 Wiley Periodicals, Inc. J Appl Polym Sci 105: 1993–1999, 2007

Key words: polyethylene (PE); organoclay; nanocomposites; mechanical properties; flame retardance

INTRODUCTION

In the past decade, polymer/clay nanocomposites have garnered considerable attention from research scientists and industries alike. Compared with conventional filled polymers, nanocomposites that contain a small amount of layered silicate, i.e., clay, demonstrate unique features such as enhanced mechanical properties, increased heat resistance, decreased gas permeability, and reduced flammability.[1–5] The key to yielding these improved properties rests in being able to exfoliate and disperse completely individual platelets with high aspect ratios (over 200) throughout the polymer matrix.

In general, interplay of entropic and enthalpic factors determines whether the nanoclay particles will exist in an intercalated or exfoliated form when dispersed within a polymer matrix.[6,7] Dispersion of clay particles in a polymer matrix requires sufficiently favorable enthalpic contributions to overcome any entropic penalty. Exfoliated nanocomposite preparation by conventional polymer processing therefore requires the occurrence of strong interfacial interactions between the polymer matrix and the clay to make the entire surface of the individual clay layers available for the polymer, as well as the generation of sufficient shear forces. This is readily achieved with high polar polymers such as polyamides.[8,9] However, for many commercially important nonpolar or weakly polar polymers such as polyethylene (PE), polypropylene, and polystyrene, the natural incompatibility with the polar clay surface pose significant challenges to achieving complete exfoliation of clays in polymer/clay nanocomposites.[10–14]

Considerable interest in polyolefin/clay nanocomposites has emerged due to their potential to offer enhanced performance at very low loadings compared with conventional filler composites in many applications, such as packaging, automobile, and other engineering applications. Especially PE is one of the largest volume thermoplastics in the world and is used widely in packaging, consumer goods, pipes, cable insulation, etc. Recent studies have focused on uniform and optimal dispersion (exfoliation) of nanosize clay platelets in the nonpolar matrix to improve their physical and mechanical properties. The most common approaches to the production of polyolefin nanocomposites involve *in situ* polymerization,[15–19] and melt compounding. The latter is more useful and convenient from an industrial standpoint, because it does not employ organic solvents and can be easily

Correspondence to: C. B. Park (park@mie.utoronto.ca).
Contract grant sponsor: Consortium for Cellular and Microcellular Plastics (CCMCP).
Contract grant sponsor: Natural Science and Engineering Research Council of Canada (NSERC).

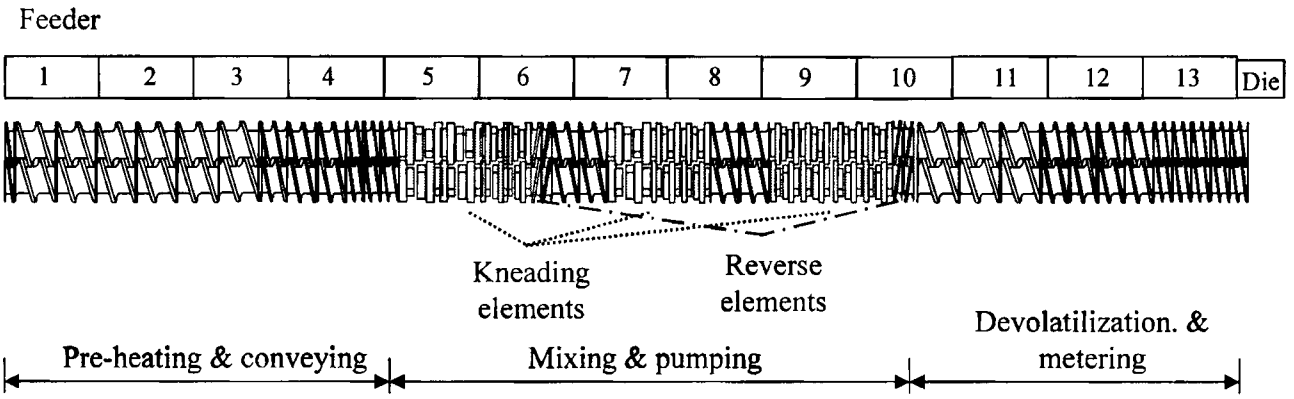

Figure 1 Screw configuration used in the corotating twin screw extruder (13 blocks).

combined with conventional polymer processes, such as extrusion and injection molding. For the melt compounding in PE/clay systems, PE functionalized via grafting of maleic anhydride or acrylic acid, as well as block-copolymers of ethylene with monomers containing acid groups have been utilized to overcome problems associated with poor interfacial interaction between polymer and filler.[20–32] Functional groups such as succinic anhydride and acids increase the associations between the clay surface and the polymer chain, providing a favorable enthalpy of mixing with the polymer matrix.

There is a vast amount of literature on PE/clay nanocomposites; however, in most cases attempts to achieve fully exfoliated clay nanocomposites adding a small amount of clay ($\sim$ 3–5 wt %) have not been successful due to the lack of favorable interactions between polymers and clay surface, resulting in clay particle aggregation. Different microstructures, including intercalated, mixed intercalated and exfoliated, ordered exfoliated, and disordered exfoliated, may be obtained depending on the clay content, with the latter being favored as the clay content decreases.[32] In intercalated nanocomposites most clay exists in layered stacks, therefore there is less actual polymer–clay interfacial contact area, whereas a completely exfoliated structure ensures maximum polymer–clay interfacial contact with their extremely fine dimensions (high aspect ratios over 200). The large surface area of fully exfoliated clay nanoparticles, and intimate contact between particles and polymer matrix may notably improve physical and mechanical properties, as well as other performance characteristics of their composites, such as flame retardancy, without affecting substantially their processability and cost, even at very low clay contents of less than 1.0 wt %. It has been reported that novel microcellular PE/clay nanocomposite foams blown with supercritical CO_2 can be obtained when less than 0.1 wt % of clay is added into a PE matrix.[33]

Accordingly, this research aims at investigating the effects of the degree of clay dispersion and exfoliation on the rheological, mechanical properties, and the flame retarding characteristics of high density polyethylene (HDPE)/clay nanocomposites containing very small amounts of clay (in the range of 0.05–1.0 wt %). A systematic study was undertaken to investigate the relative influence of clay structure (i.e., aggregated/intercalated versus completely exfoliated) on the properties of the matrix material.

EXPERIMENTAL

Materials

In this study, HDPE (2607; Nova Chemicals, Calgary, Canada) with a density of 0.947 g/cm^3 and a melt flow index (MFI) of 5.0 g/10 min (ASTM D 1238) and HDPE-*g*-maleic anhydride (PE-*g*-MAn, Fusabond MB-100D, MFI = 0.96; DuPont Canada, Kingston, Canada) were used. An organoclay, natural montmorillonite layered silicate modified with dimethyl dehydrogenated tallow alkyl ammonium (Cloisite 20A; Southern Clay Products, Gonzales, TX) was utilized as a filler.

Preparation and characterization of HDPE/clay nanocomposites

All nanocomposites were prepared using a ZSK-30 Werner Pfleiderer intermeshing and corotating twin-screw extruder, having a 30 mm screw diameter and L/D 40 : 1. The screw configuration used in this study had three kneading block sections and two reverse sections (Fig. 1) to improve the mixing and ensure sufficient residence time for good dispersion of clay particles. The screw speed was 20 rpm. The extrusion temperatures were controlled at 180°C. These conditions resulted in a mean residence time of 300–320 s.

A first series of composites, comprising HDPE/clay composites containing 0.05, 0.5, and 1.0 wt % clay, were prepared by direct melt compounding and are denoted as HNC0.05–HNC1.0. The second series of composites contained HDPE, PE-*g*-Man, and clay; the PE-*g*-MAn content was kept constant to 50 wt %. Based on our previous work, this amount of PE-*g*-MAn can generate fully exfoliated structures. Nano-

composites containing 1, 3, and 5 wt % clay (denoted as HWC1.0, 3.0, and 5.0, respectively) were prepared by directly melt compounding all components. As an example HWC1.0 stands for a composite containing HDPE/PE-*g*-MAn/Clay (49/50/1) by weight. Composites containing 0.05–0.5% were prepared by further dilution of the composite containing 1 wt % clay, with appropriate amounts of HDPE and PE-*g*-MAn.

The nanocomposite structure was characterized by wide-angle X-ray diffraction (XRD) and transmission electron microscopy (TEM). XRD was conducted with a Siemens D5000 diffractometer using Cu Kα radiation (1.5478 Å) with a Kevex solid-state detector. Measurement was performed at 50 kV and 35 mA. The data was recorded in the reflection mode in the range of $2\theta = 1.0–10^\circ$ using the STEP scan mode; the step size was 0.02° and the counting time was 2.0 s per step. Materials with periodic structure like the layered silicate clays show characteristic (001) diffraction peaks, which are related to the spacing of the layers according to Bragg's law, $\lambda = 2d_{001} \sin\theta$, where λ is the wavelength of the radiation, d_{001} is the interlayer distance, and 2θ is the diffraction angle. For the TEM analysis, the specimen was prepared as an ultrathin section of 70 nm thickness using an ultracryo-microtome with a diamond knife at -100°C. The structure was observed using a FEI Technai 20 (Phillips) microscope at 200 kV.

Rheological characterization

Samples for rheological characterization were disks of 25 mm diameter and 2 mm thickness, which were prepared by compression molding at 170°C. The samples were subjected to oscillatory shear in a Dynamic Stress Rheometer (SR-200; Rheometric Scientific) with parallel plates (25 mm in diameters) and at a gap of 1.0 mm. In all the cases, dynamic strain sweeps were initially performed to define the limits of the linear viscoelastic regime. Dynamic frequency sweep experiments were then conducted to measure the storage modulus (G'), loss modulus (G''), and complex viscosity (η^*) over a frequency range of 0.1–100 rad/s at 190°C. All measurements were performed under nitrogen to prevent polymer degradation or moisture absorption.

Mechanical property testing

Tensile property tests were performed using a Sintech model 20 at a crosshead speed of 100 mm/min at room temperature according to ASTM D 638. Sheets with a thickness of 3 mm were prepared by compression molding at 170°C, from which test specimens were cut using a Type V die. Five measurements per each sample were taken checking the repeatability of data.

Flame retardance test

The flame retardancy test was carried out according to ASTM D 635. Sheets with a thickness of 3.0 mm were prepared by compression molding at 170°C, from which test specimens were cut. The dimensions of the specimens used are 127 mm in length, 12.7 mm in width, and 3.0 mm in thickness.

The burning rate is calculated according to the formula:

$$B = 60 \times \frac{D}{T} \quad (1)$$

where B is the burning rate in millimeter per minute, D is the length the flame travels (75 mm), and T is the time in seconds for the flame to travel D mm. Five measurements per each sample were taken for checking the repeatability of data.

RESULTS AND DISCUSSION

Structure of nanocomposites

Figures 2 and 3 show the XRD patterns for nanocomposites containing different clay contents. XRD patterns of the composites containing PE-*g*-MAn are presented in Figure 2. In the case of HWC1.0, there were no characteristic clay peaks, indicating that an exfoliated structure was achieved. For HWC3.0 and HWC5.0, there was a substantial reduction in the intensity of the diffraction peak, which is shifted at a lower angle than that of pure clay, suggesting a mixture of intercalated and exfoliated clay. It is apparent therefore that, under the same processing conditions, clay concentration affects the degree of the exfoliation. No evidence of a peak was seen at clay loadings below

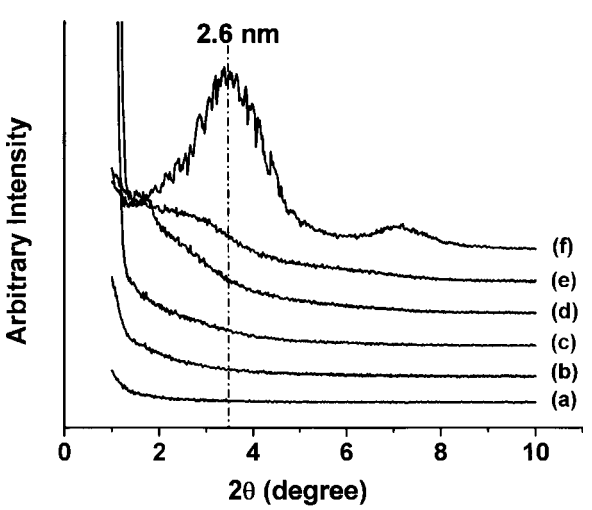

Figure 2 X-ray diffraction patterns of HWC composites: (a) HWC0.05, (b) HWC0.5, (c) HWC1.0, (d) HWC3.0, (e) HWC5.0, (f) pure clay (Cloisite 20A).

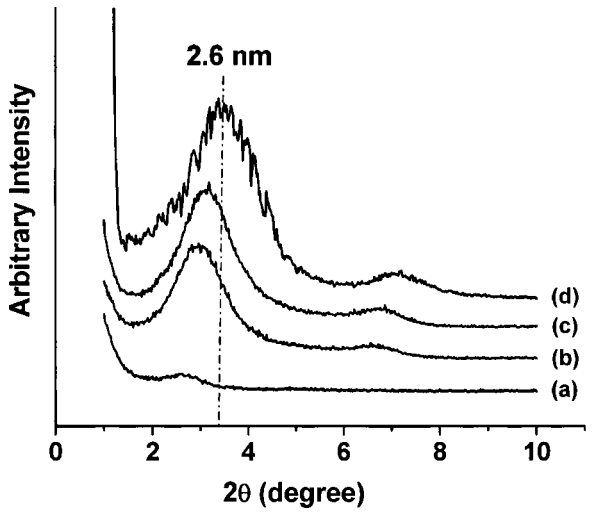

Figure 3 X-ray diffraction patterns of HNC composites: (a) HNC0.05, (b) HNC0.5, and (c) HNC.1.0, (d) pure clay (Cloisite 20A).

1 wt %. The successful generation of exfoliated structures is attributed largely to the chosen screw configuration, which ensured increased residence time and moderately high shear intensity inside the extruder, thereby facilitating the diffusion of polymer into the clay galleries. In addition to the choice of suitable processing conditions, increasing the compatibility between the matrix and the organoclay by adding PE-*g*-MAn is necessary to facilitate delamination of clay platelets. Figure 3 presents that XRD patterns of HNC composites exhibit intercalated structures as clearly indicated by the presence of intense characteristic clay peaks shifted slightly to lower angles.

The morphology was further examined using TEM. Figure 4 shows the TEM images of some nanocomposites, which correspond to the XRD patterns presented in Figures 2 and 3. In the case of the HWC composites, the delaminated silicate layers are dispersed uniformly in the HDPE matrix, whereas HNC composites show stacked silicate tactoids of about 300–500 nm length and about 50–200 nm thickness. The presence of tactoids in the TEM images of HNC composites corroborates the XRD findings and suggests the presence of a mixture of aggregated and intercalated structures. In the absence of PE-*g*-MAn, the clay aggregates have been sheared off and broken down into large stacks. Dennis et al.[9] stated that in the presence of PE-*g*-MAn the primary clay particles (aggregates) are first fractured by mechanical shear in the extruder. The PE-*g*-MAn chains then diffuse into the clay galleries because of either a physical or chemical affinity between the polymer and the organoclay surface and push the platelets apart. After this, an onion-like delaminating process continues to disperse the platelets into the HDPE matrix. The diffusion of polymer into the clay galleries is facilitated by increased residence time in the extruder; therefore, potentially processing could be optimized to ensure exfoliation in the case of the nanocomposites.

Rheological properties

It is commonly accepted that adding nanosized clay particles into pure polymer changes the rheological properties of the polymer matrix.[24–26,28–32,34,35] The rheological properties of polymer/clay nanocomposites are of particular importance, because they relate to their microstructure and determine their processibility. Figure 5 shows the effect of clay dispersion on the complex viscosity (η*) of HDPE/clay nanocomposites with different content of clay. The complex viscosity of pure HDPE and all HNC nanocomposites show only mild frequency dependence with a Newtonian plateau at low angular frequencies in oscillatory shear flow. There is virtually no enhancement in the melt viscosity of HNC composites containing small amounts of clay (0.05–1.0 wt %). Turning to the HWC-series of nanocomposites, HWC0.0, which is basically the polymer matrix of HWC composites, also shows Newtonian behavior at low frequencies; it should be noted that the complex viscosity of HWC0.0, which essentially comprises of an HDPE/PE-*g*-MAn blend, is higher than that of pure HDPE, obviously due to the higher viscosity (lower MFI) of PE-*g*-MAn. However η* of all HWC nanocomposites exhibits a further pronounced increase at low frequencies accompanied by increasingly shear thinning behavior. Such a behavior can be explained based on the surface area of particulates. The smaller the size of particulates (thus

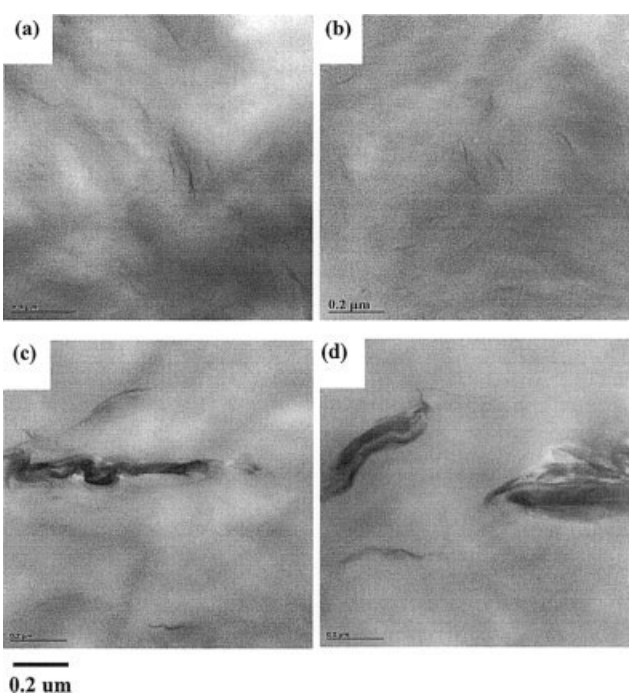

Figure 4 TEM micrographs of (a) HWC0.5, (b) HWC1.0, (c) HNC0.5, and (d) HNC1.0.

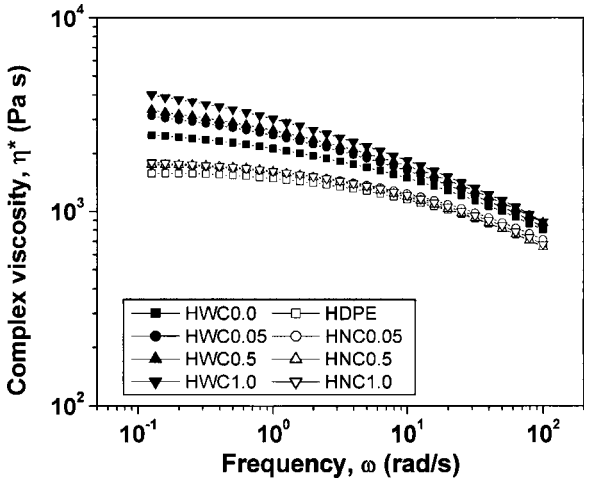

Figure 5 The effects of clay dispersion and content on the complex viscosity (η*) for HDPE/clay nanocomposites in the presence (filled symbols) and absence (open symbols) of PE-*g*-MAn with different content of clay.

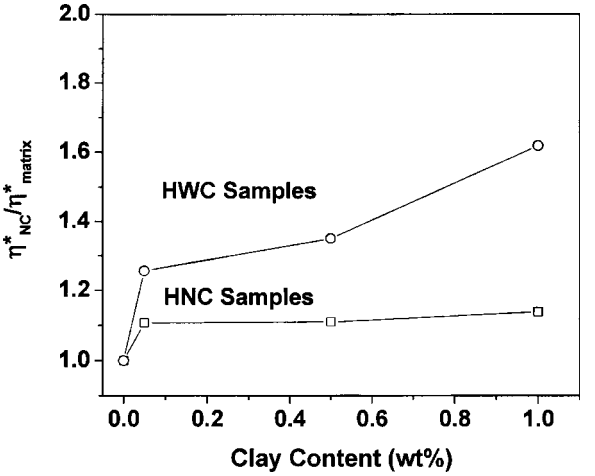

Figure 6 The ratio of complex viscosity of HNC and HWC composites (η^*_{NC}) over polymer matrix viscosity (η^*_{matrix}) at a frequency (ω) of 0.12 rad/s.

the larger their surface area) in a composite, the lower will be the content that can give rise to shear thinning.[22] The effect of clay dispersion and exfoliation on the complex viscosity is readily identified in Figure 6. The relative viscosity ratio of HWC samples shows a steeper increase as a function of clay content than that of HNC samples. Generally, the ratio of complex viscosities depends on the content, size, shape, and stiffness of fillers.[36,37] In this study, the aspect ratio of clay particles dispersed in the polymer matrix plays an important role. The high aspect ratio and large surface area of exfoliated clay particles is responsible for the higher ratio of relative viscosities observed in Figure 6. In other words, the higher the degree of clay particles dispersion in the HDPE matrix the larger the interfacial area between the components (the aspect ratio of silicate nanoplatelets is high). This causes a higher fraction of polymer chains to be confined by nanoplatelets; therefore, their mobility is restricted.

Figure 7 shows the effect of clay dispersion on the storage modulus (G') of HDPE/clay nanocomposites containing different amounts of clay. Consistently with the complex viscosity results, the G' of the HWC0.0 matrix is higher than that of HDPE, but at low frequencies it still approaches a terminal slope of 2. G' of all HWC composites further exhibits a monotonic increase with increasing clay content from 0 to 1.0 wt % at all frequencies. However, an increase in the content of clay has little effect on the G' of HNC composites over the entire range of angular frequencies (ω) investigated. Moreover, in the terminal region, the slope of G' decreases slightly with increasing clay content ranging from 0.05 to 1.0 wt % for HWC composites and becomes close to 1. However, the slope of HNC composites, which is close to 2, is independent of clay content; such linear dynamic viscoelastic behavior is expected for unfilled homopolymers. The behavior of HWC composites is attributable to the increased number and surface areas of exfoliated clay platelets due to an enhanced dispersion of clay aggregates.

Tensile properties

Table I summarizes the tensile moduli, strength, and strain at yield for HDPE nanocomposites with and without PE-*g*-MAn as a function of clay content. The tensile moduli and tensile strength are further plotted as a function of clay content in Figure 8. For the HWC samples, whose matrix comprises of a mixture of HDPE and PE-*g*-MAn, a modest increase in yield strength and a pronounced increase in tensile modu-

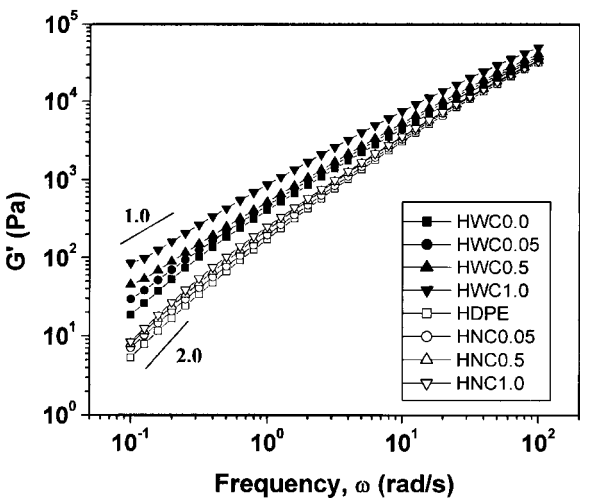

Figure 7 The effects of clay dispersion and content on the storage modulus (G') for HDPE/clay nanocomposites in the presence (filled symbols) and absence (open symbols) of PE-*g*-MAn with different content of clay.

TABLE I
Effects of Clay Dispersion and Content on the Tensile Modulus, Strength, and Yield Strain of HDPE/Clay Nanocomposites

Clay content (wt %)	Tensile modulus (MPa)		Yield strength (MPa)		Yield strain (%)	
	HNC	HWC	HNC	HWC	HNC	HWC
0.0	177	213	18.6	20.8	21.2	17.7
0.05	186 (+5.1)	254 (+19.2)	19.1 (+2.7)	21.7 (+4.3)	17.5 (−17.5)	16.6 (−6.2)
0.5	193 (+9.0)	259 (+21.6)	19.1 (+2.7)	21.9 (+5.3)	17.3 (−18.4)	15.7 (−11.3)
1.0	197 (+11.3)	270 (+26.8)	19.2 (+3.2)	22.2 (+6.7)	16.4 (−22.6)	15.2 (−14.1)
3.0	–	278 (+30.5)	–	22.5 (+8.2)	–	14.1 (−20.3)
5.0	–	295 (+38.5)	–	23.6 (+13.5)	–	12.5 (−29.4)

Numbers in parentheses refer to the difference (in %) between a base material and the composites.

lus over the base material are observed upon addition of extremely low amounts of clay (0.05 wt %). The values level off above this clay loading and exhibit a further pronounced increase when the clay content is higher than 1 wt %.

The respective HNC composites, containing mixtures of aggregated and intercalated structure, only showed minor increases in tensile properties. It is clear therefore that the essential factor governing the enhancement of mechanical properties in the nanocomposites is the enhanced interfacial contact between polymer and clay, generated by the high aspect ratio of the dispersed clay particles.[29,38,39] This leads to better stress transfer at the interface between the HDPE matrix and the clay particles.

In all composites the yield strain decreased with increasing clay loading, indicating increasing brittleness for the composites. However, the decrease in yield strain is more pronounced for the HNC series of composites, suggesting that presence of clay in an exfoliated state is less detrimental for the ductility of the material.

Flame retardance

To understand how the structure of nanocomposites influences their flammability, the exfoliated nanocomposites (HWC-series) were compared with their intercalated counterparts (HNC-series). Figure 9 shows a reduction in the burning rate (by as much as 10–15%) for exfoliated HDPE nanocomposites over the unfilled

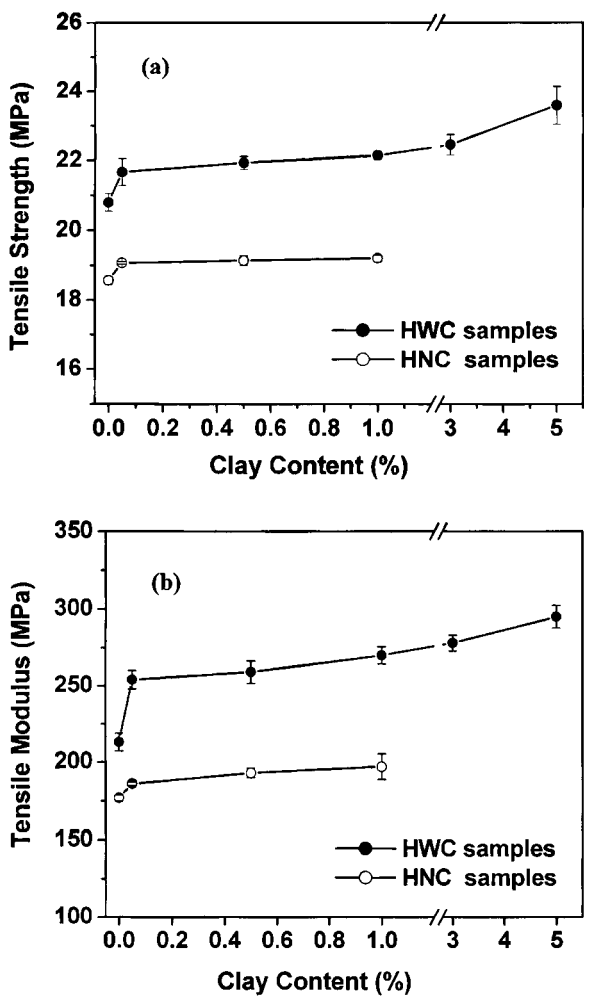

Figure 8 The effects of clay dispersion and content on (a) tensile strength and (b) tensile modulus for HDPE/clay nanocomposites.

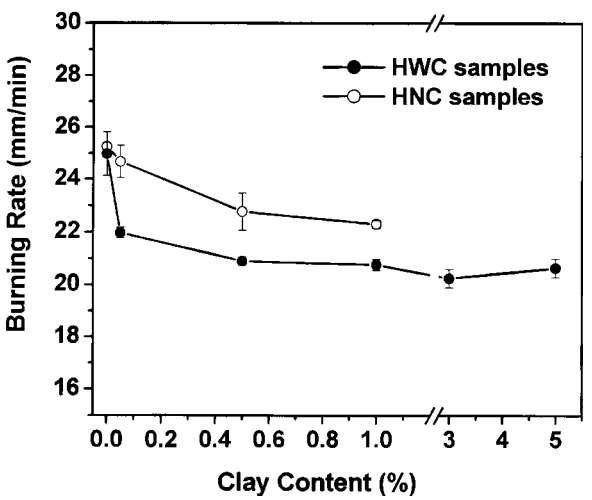

Figure 9 The effects of clay content and dispersion on the burning rate of HDPE/clay nanocomposites with and without PE-*g*-MAn.

neat material at clay levels below 1.0 wt %, indicating that their flame retardant performance was improved. However, only marginal reductions were observed for HNC composites. In consequence, it can be argued that achieving a higher degree of exfoliation for the nanosized clay is pivotal for enhancing the flame retarding properties of materials when a very small amount of clay is used. Exfoliated clay platelets may insulate the underlying material and slow the mass loss rate of decomposition products. This finding is in agreement with a recent study by Gilman et al.,[40] who reported that the clay particles must be dispersed at the nanoscale level to affect the flammability of the nanocomposites.

CONCLUSIONS

This study provided evidence that an important and challenging task in realizing the advantages of the addition of nanosized clay particles into polymer lies in ensuring the uniform dispersion of the high aspect ratio crystal-like platelets in the polymer matrix.

Fully exfoliated HDPE/clay nanocomposites were successfully achieved by melt blending under suitable compounding conditions, with the aid of maleated PE. The rheological, mechanical properties, and flame retardancy of HDPE nanocomposites were affected by the content and the degree of exfoliation of the nanoclay. In particular, fully exfoliated nanocomposites with good nanoscale dispersion of clay platelets showed remarkable improvements in rheological, tensile modulus, and flame retardancy over their unfilled base material even at very small levels of clay (0.05–1.0 wt %), when compared with those containing mixtures of aggregated and intercalated clay. In consequence, it was demonstrated that achieving a higher degree of exfoliation for nanosized clay particles is key to enhancing the rheological, mechanical, and flame retarding properties even when small amounts of clay (only less than 1%) are used.

The authors thank DuPont Canada and Nova Chemicals for supplying materials.

References

1. Giannelis, E. P. Adv Mater 1996, 8, 29.
2. Krishnamoorti, E.; Vaia, R. A.; Giannelis, E. P. Chem Mater 1996, 8, 1718.
3. Kojima, Y.; Usuki, A.; Kawasumi, M.; Okada, A.; Fukushima, Y.; Kurauchi, T.; Kamigaito, O. J Mater Res 1993, 8, 1185.
4. Wang, K. H.; Chung, I. J.; Jang, M. C.; Keum, J. K.; Song, H. H. Macromolecules 2002, 35, 5529.
5. Wang, K. H.; Xu, M.; Choi, Y. S.; Chung, I. J. Polym Bull 2001, 46, 499.
6. Vaia, R. A.; Giannelis, E. P. Macromolecules 1997, 30, 7990.
7. Vaia, R. A.; Giannelis, E. P. Macromolecules 1997, 30, 8000.
8. Usuki, A.; Kojima, Y.; Kawasumi, M.; Okada, A.; Fukushima, Y.; Kurauchi, T.; Kamigaito, O. J Mater Res 1993, 8, 1179.
9. Dennis, H. R.; Hunter, D. L.; Chang, D.; Kim, S.; White, J. L.; Cho, J. W.; Paul, D. R. Polymer 2001, 42, 9513.
10. Tanoue, S.; Utracki, L. A.; Garcia-Rejon, A.; Tatibouet, J.; Cole, K. C.; Kamal, M. R. Polym Eng Sci 2004, 44, 1046.
11. Ton-That, M. T.; Perrin-Sarazin, F.; Cole, K. C. Polym Eng Sci 2004, 44, 1212.
12. Sepehr, M.; Utracki, L. A.; Zheng, X.; Wilkie, C. A. Polymer 2005, 46, 11569.
13. Perrin-Sarazin, F.; Ton-That, M. T.; Bureau M. N.; Denault, J. Polymer 2005, 46, 11624.
14. Ton-That, M. T.; Tsai, S. J. Polym Eng Sci 2006, 46, 1061.
15. Osman, M. A.; Rupp, J. E. P.; Suter, U. W. Polymer 2005, 46, 1653.
16. Alexandre, M.; Dubois, P.; Sun, T.; Garces, I. M.; Jerome, R. Polymer 2000, 43, 2123.
17. Bergman, J. S.; Chen, H.; Giannelis, E. P.; Thomas, M. G.; Coates, T. G. Chem Commun 1999, 21, 2179.
18. Heinemann, J.; Reichert, P.; Thomann, R.; Mulhaupt, R. Macromol Rapid Commun 1999, 20, 423.
19. Xu, J. T.; Zhao, Y. Q.; Wang, Q.; Fan, Z. Q. Polymer 2005, 46, 11978.
20. Saul, S. V.; Maria, L. L. Q.; Eduardo, R. V.; Francisco, J. M. R.; Juan, M. G. R. Macromol Mater Eng 2006, 291, 128.
21. Truss, R. W.; Yeow, T. K. J Appl Polym Sci 2006, 100, 3044.
22. Osman, M. A.; Rupp, J. E. P.; Suter, U. W. Polymer 2005, 46, 8202.
23. Xu, Y.; Fang, Z.; Tong, L. J Appl Polym Sci 2005, 96, 2429.
24. Chrissopoulou, K.; Altintzi, I.; Anastasiadis, S. H.; Giannelis, E. P.; Pitsikalis, M.; Hadjichristidis, N.; Theophilou, N. Polymer 2005, 46, 12440.
25. Lee, Y. H.; Park, C. B.; Wang, K. H. J Cell Plast 2005, 41, 487.
26. Lee, J. A.; Kontopoulou, M.; Parent, J. S. Polymer 2004, 45, 6595.
27. Liang, G.; Xu, J.; Bao, S.; Xu, W. J Appl Polym Sci 2004, 91, 3974.
28. Hotta, S.; Paul, D. R. Polymer 2004, 45, 7639.
29. Kato, M.; Okamoto, H.; Hasegawa, N.; Tsukigase, A.; Usuki, A. Polym Eng Sci 2003, 43, 1312.
30. Gopakumar, T. G.; Lee, J. A.; Kontopoulou, M.; Parent, J. S. Polymer 2002, 43, 5483.
31. Koo, C. M.; Ham, H. T.; Kim, S. O.; Wang, K. H.; Chung, I. J.; Kim, D. C.; Zin, W. C. Macromolecules 2002, 35, 5116.
32. Koo, C. M.; Kim, S. O.; Chung, I. J. Macromolecules 2003, 36, 2748.
33. Lee, Y. H.; Wang, K. H.; Park, C. B.; Sain, M. J. Appl Polym Sci 2007, 103, 2129.
34. Ren, J. A.; Silva, S.; Krishnamoorti, R. Macromolecules 2000, 39, 3979.
35. Lee, K. M.; Han, C. D. Polymer 2003, 44, 4573.
36. Hoffman, B.; Dietrich, C.; Thomann, R.; Friedrich, C.; Mulhaupt, R. Macromol Rapid Commun 2000, 21, 57.
37. Shenoy, A. V. Rheology of Filled Polymer System; Kluwer Academic, Dorecht: Boston, 1999.
38. Nielsen, L. E. Mechanical Properties of Polymer and Composites, Vol. 2; Marcel Dekker: New York, 1981.
39. Shang, S. W.; Willams, J. W.; Soderholm, K. J. M. J Mater Sci 1994, 29, 2406.
40. Gilman, J. W.; Jackson, C. L.; Morgan, A. B.; Harris, J. R.; Manias, E.; Giannelis, E. P.; Wuthenow, M.; Hilton, D.; Philips, S. H. Chem Mater 2000, 12, 1866.